

On the Astrometric Behavior of Binary Microlensing Events

Cheongho Han

Department of Astronomy & Space Science, Chungbuk National University, Chongju,
Korea 361-763; cheongho@astro.chungbuk.ac.kr

ABSTRACT

Despite the suspected binarity for a significant fraction of Galactic lenses, the current photometric surveys detected binary microlensing events only for a small fraction of the total events. The detection efficiency is especially low for non-caustic crossing events, which comprise majority of the binary lensing events, due to the absence of distinctive features in their light curves combined with small deviations from the standard light curve of a single point-mass event. In addition, even they are detected, it will be difficult to determine the solution of the binary lens parameters due to the severe degeneracy problem. In this paper, we investigate the properties of binary lensing events expected when they are astrometrically observed by using high precision interferometers. For this, we construct vector field maps of excess centroid shifts, which represent the deviations of the binary lensing centroid shifts from those of a single lensing events as a function of source position. From the analysis of the maps, we find that the excess centroid shifts are substantial in a considerably large area around caustics. In addition, they have characteristic sizes and directions depending strongly on the source positions with respect to the caustics and the resulting trajectories of the light centroid (astrometric trajectories) have distinctive features, which can be distinguished from the deviations caused by other reasons. We classify the types of the deviations and investigate where they occur. Due to the strong dependency of the centroid shifts on the lens system geometry combined with the distinctive features in the observed astrometric trajectories, astrometric binary lensing observations will provide an important tool that can probe the properties of Galactic binary lens population.

Subject headings: gravitational lensing – binaries: general – astrometry

1. Introduction

Searches for Galactic dark matter by monitoring light variations of stars located in the Magellanic Clouds and Galactic bulge caused by gravitational microlensing have been or are being carried out by several groups (MACHO: Alcock et al. 2000; EROS: Afonso et al. 1999; OGLE: Udalski, Kubiak, & Szymański 1997). The searches have been very successful and the total number of candidate events now reaches up to 1,000 (P. Popowski 2000, private communication). Among these events, a notable fraction of events are believed to be caused by binary lenses (Udalski et al. 1994; Bennett et al. 1995; Alard, Mao, &

Guibert 1995; Rhie & Bennett 1996; Pratt et al. 1996; Albrow et al. 1996; Dominik & Hirshfeld 1996; Alcock et al. 1999a, 1999b). Detecting binary lensing events is important because one can obtain valuable information about Galactic binary lens population such as the distributions of binary mass ratios and separations.

Due to the difference in the lens system geometry, the light curve of a binary lensing event deviates from the single-peak symmetric one of an event caused by a single point-mass lens. The most important difference in the geometry of a binary lens system from that of a single lens system is the formation of caustics. When a source star crosses the caustics, an extra pair of images appear (or disappear) and its flux is greatly amplified, resulting characteristic sharp spikes in the light curve. If the source does not cross the caustics, on the other hand, the light curve is less perturbed and in most cases has no distinctive features such as the spikes of the caustic crossing event. Di Stefano & Perna (1997) pointed out that the detection efficiency of non-caustic crossing binary lensing events is significantly lower than that of caustic crossing events due to the absence of distinctive features in their light curves combined with small deviations. This was well demonstrated by the recent MACHO result where non-caustic crossing events comprise only $\sim 25\%$ of the total detected binary lensing events despite their predicted higher frequency of occurrence (Alcock et al. 1999b). Another problem in investigating binaries from microlensing is that even if an event is detected, it is difficult to determine the solution of the binary lens parameters, especially for non-caustic crossing events, due to the severe degeneracy problem (Mao & Di Stefano 1995). The level of degeneracy is so high for most gently perturbed light curves of non-caustic crossing events that many of these events allow fits to models of the binary companion ranging from equal-mass binary to planets (Di Stefano & Perna 1997). Although the level of degeneracy for caustic crossing events is relatively low due to the characteristic spike feature in their light curves, they cannot be totally free from the degeneracy problem (Dominik 1999; Albrow et al. 1999). Therefore, for the acquisition of accurate information about Galactic binaries from microlensing, it will be essential to devise a new method that can effectively detect binary lensing including non-caustic crossing events and can resolve their degeneracy problem.

In addition to photometry, microlensing can also be detected and observed astrometrically. When a source star is lensed by a single point-mass lens, its image is split into two. The typical separation between the two images for a Galactic event caused by a stellar mass lens is on the order of a milli-arcsec. This separation is too small for direct observation of the individual images even with the *Hubble Space Telescope*. However, if microlensing is observed by using several planned high-precision interferometers from space-based platform, e.g. the *Space Interferometry Mission* (SIM, <http://sim.jpl.nasa.gov>), and ground-based large telescopes, e.g. the Keck and the Very Large Telescope, one can measure the astrometric displacements in the source star image light centroid, $\delta\theta_c$. Once the centroid shifts are measured and their trajectory is constructed, one can determine the lens proper motion, from which one can better constrain the lens mass compared to the photometrically obtained Einstein ring radius crossing time t_E . Astrometric microlensing observation was first proposed nearly simultaneously by Miyamoto & Yoshii (1995), Høg, Novikov, & Polnarev (1995), and Walker (1995) and further analysis considering actual

performances of specific instrument has been done by Boden, Shao, & Van Buren (1998). A modified idea of monitoring a nearby high proper motion star working as a lens instead of monitoring a source star for the accurate determination of the lens mass was proposed by Miralda-Escudé (1996) and Paczyński (1998). For a single lensing event, the light centroid traces out an elliptical trajectory during the event (Walker 1995; Jeong, Han, & Park 1999). If an event is caused by a binary, on the other hand, the resulting trajectory of the light centroid (astrometric trajectory) deviates from the elliptical one of the single lensing event (Chang & Han 1999), which is analogous to the deviations in the photometric light curve.

In this paper, we investigate the properties of binary lensing events when they are astrometrically observed by using high precision interferometers. For this, we construct vector field maps of excess centroid shifts, $\Delta\delta\theta_c(\xi, \eta)$, which represent the deviations of the binary lensing centroid shifts from those of a single lensing event as a function of source position $\zeta = (\xi, \eta)$. From the analysis of the maps, we find that the excess centroid shifts are substantial in a considerably large area around caustics. In addition, they have characteristic sizes and directions depending strongly on the source positions with respect to the caustics and the resulting astrometric trajectories have distinctive features which can be distinguished from the deviations caused by other reasons. We classify the types of the deviations and investigate where they occur.

2. Basics of Binary Lensing

When lengths are normalized to the combined Einstein ring radius, the lens equation in complex notations for a binary lens system is represented by

$$\zeta = z + \frac{m_1}{\bar{z}_1 - \bar{z}} + \frac{m_2}{\bar{z}_2 - \bar{z}}, \quad (1)$$

where m_1 and $m_2 = 1 - m_1$ are the mass fractions of the individual lenses, z_1 and z_2 are the positions of the lenses, $\zeta = \xi + i\eta$ and $z = x + iy$ are the positions of the source and images, and \bar{z} denotes the complex conjugate of z (Witt 1990). The combined Einstein ring radius is related to the total mass and the location of binary the lens by

$$r_E = \left(\frac{4GM}{c^2} \frac{D_{ol}D_{ls}}{D_{os}} \right)^{1/2}, \quad (2)$$

where D_{ol} , D_{ls} , and D_{os} represent the separations between the observer, lens, and source star, respectively. For a binary lensing event, the number of images is either three or five depending on the source position. The amplifications of the individual images are given by the Jacobian of the transformation (1) evaluated at the image position, i.e.

$$A_i = \left(\frac{1}{|\det J|} \right)_{z=z_i}; \quad \det J = 1 - \frac{\partial\zeta}{\partial\bar{z}} \frac{\partial\bar{\zeta}}{\partial z}. \quad (3)$$

The caustic refers to the source position on which the amplification of a point source event becomes infinity, i.e. $\det J = 0$. The total amplification is given by the sum of the

amplifications of the individual images, i.e. $A = \sum_i A_i$. Since the position of the image centroid equals to the amplification weighted mean position of the individual images, the source image centroid shift with respect to the unlensed source position is given by

$$\delta\theta_c = \frac{\sum_i A_i z_i}{\sum_i A_i} - \zeta, \quad (4)$$

where the positions of the individual images z_i are obtained by numerically solving the lens equation (1).

3. Properties of Various Types of Binary Lensing Events

The size of caustics depends strongly on the binary separation ℓ (normalized by the combined angular Einstein ring radius $\theta_E = r_E/D_{ol}$), causing strong dependency of the caustic crossing probability on the binary separation. Caustic crossing is optimized when the binary separation is equivalent to the angular Einstein ring radius. Han (1999) estimated that when the binary separation is in the range $0.7 \lesssim \ell \lesssim 1.8$, the caustic crossing probability is greater than $\sim 50\%$.¹ However, as the separation further increases or decreases, the caustic crossing probability decreases rapidly. Therefore, most non-caustic crossing events are caused by binaries with separations either substantially smaller (narrow binaries) or larger (wide binaries) than θ_E . In this work, we focus on the astrometric properties of events caused by these types of binary lenses because they are much more common.

3.1. Narrow Binary Lensing Events

If an event is caused by a narrow binary, the lens system forms 3 separated closed caustics. One of them is located near the center of mass (the central caustic) and has a diamond shape with 4 cusps. The other two are located away from the center of mass (the outer caustics) and each of them has a wedge-like shape with 3 cusps. The outer caustics are symmetric with respect to the binary axis and are located on the heavier lens side with respect to the center of mass. Compared to the central caustic, the outer caustics are much smaller (see Figure 1). If the binary separation is very small, both the central and outer caustics become very small and the geometry of the lens system mimics that of a single lensing event with a mass equal to the total mass of the binary and located at the center of mass of the binary (Gaudi & Gould 1997). For a narrow binary lensing event, we, therefore, define the *excess centroid shift* by

$$\Delta\delta\theta_c = \delta\theta_{c,b} - \delta\theta_{c,s}, \quad (5)$$

¹He estimated the probability under the definition of a binary lensing event as ‘a close lens-source encounter within the combined Einstein ring radius with its center at the center of mass of the binary lens system’.

where $\delta\theta_{c,b}$ and $\delta\theta_{c,s}$ represent the centroid shifts of the binary and the corresponding single lensing event, respectively.

In Figure 1, we present the vector field map of the excess centroid shifts, $\Delta\delta\theta_c(\xi, \eta)$, for an example narrow binary lens system with $\ell = 0.5$ and $q = 0.2$. The positions in the map are chosen so that the center of mass of the binary is at the origin. Both lenses are located on the ξ axis and the heavier lens is to the right. The circle drawn with a long-dashed line represents the combined Einstein ring and the closed figures drawn by thick solid line are caustics. Also drawn on the map are the contours of the absolute value of the excess centroid shift, $\Delta\delta\theta_c$. The contours are drawn at the levels of $\Delta\delta\theta_c = 0.02\theta_E$ (dotted line) and $0.2\theta_E$ (solid line). The angular Einstein ring radius of a Galactic bulge event caused by a stellar mass lens with $M \sim 0.3 M_\odot$ located at the half way between the observer and the source, i.e. $D_{ol}/D_{os} = 0.5$, is $\theta_E \sim 300 \mu\text{-arcsec}$. Therefore, these thresholds correspond to $\Delta\delta\theta_c \sim 6 \mu\text{-arcsec}$ and $\Delta\delta\theta_c \sim 60 \mu\text{-arcsec}$, which are respectively related to the astrometric precisions of the SIM (Unwin et al. 1997) and the interferometers on the large ground-based telescopes (Colavita et al. 1998; Mariotti et al. 1998). To better show $\Delta\delta\theta_c(\xi, \eta)$ near the caustic regions, we expand map of the regions and presented in Figure 2: upper panel for the central caustic region and lower panel for the outer caustic region. In Figure 3, we also present the light curves (upper 6 panels) and the astrometric trajectories (lower 6 panels) for several example non-caustic crossing events whose source trajectories are marked in Figure 1a (straight lines with arrows). Note that the number in each panel of Fig. 3 matches with the number of the corresponding source trajectory in Fig. 1.

From the analysis of $\Delta\delta\theta_c(\xi, \eta)$ in various regions outside the caustics² and the resulting light curves and astrometric trajectories, one finds the following patterns of the excess centroid shifts. First, as already known by Chang & Han (1999), the amount of excess centroid shifts is substantial in a considerably large area around caustics, c.f. the excess amplification map of Gaudi & Gould (1997), implying that astrometric binary lensing observation is an efficient method in detecting non-caustic crossing events caused by narrow binary lenses.³ The excess centroid shifts are especially large in the regions along the binary axis and the lines connecting the central and outer caustics. In the region along the binary axis, the excess centroid shifts diverges from the on-binary-axis cusps of the central caustic. Then, if a source passes through this region (e.g. the source trajectories 4 and 5), the resulting astrometric trajectory becomes *convex* compared to the elliptical one of the corresponding single lensing event. By contrast, in the regions along the lines connecting the central and outer caustics, the excess centroid shifts converge towards the

² Since our major interest is the astrometric properties of non-caustic crossing events, in this section we limit our discussion only about excess centroid shifts in the regions outside of caustics. The properties of $\Delta\delta\theta_c$ in the region inside of caustics will be discussed in § 3.3

³ It would be useful to estimate the average amount of deviation expected from a typical Galactic event. For this estimation, it is required to know not only the physical distributions of Galactic binaries and their mass function but also the distributions of their mass ratios and separations. However, our knowledge about these quantities are very poor and thus we just compare the expected deviation for events caused by an example binary lens system.

off-binary-axis cusps of the central caustic. Then, the astrometric trajectory of an event with a source trajectory passing through this region (e.g. the source trajectories 1, 2, and 3) will become *concave* with respect to that of the corresponding single lensing event or even *twisted*. Due to these various types of deviations, the astrometric trajectories of non-caustic crossing binary lensing events have distinctive features. By contrast, the light curves in most cases have no strong characteristic features.

3.2. Wide Binary Lensing Events

If an event is caused by a wide binary, on the other hand, the lens system forms 2 separate closed caustics, which are located close to the individual lenses along the binary axis. Each caustic has a wedge-like shape with 4 cusps (see Figure 4). For an event caused by these systems, the observed light curve and the astrometric trajectory appear to be the superpositions of those resulting from two events in which the component lenses behave as if they are two independent single lenses (Di Stefano & Mao 1996; Di Stefano & Scalzo 1999; An, Han, & Park 2000). Therefore, we define the excess centroid shifts of a wide binary lensing event by

$$\Delta\delta\theta_c = \delta\theta_{c,b} - \delta\theta_{c,s,comb}, \quad (6)$$

where the combined centroid shift $\delta\theta_{c,s,comb}$ represents the vector sum of the centroid shifts caused by the individual single lenses.

In Figure 4, we present excess centroid shift map for an example wide binary lens system with $\ell = 2.0$ and $q = 0.5$. In the figure, the two circles in the map drawn with a long-dashed line represent the Einstein rings of the individual single lenses. Besides that there are two Einstein rings, the positions and notations are same as those in Fig. 1. Maps in the regions around caustics are presented in Figure 5. In Figure 6, we also present the light curves and astrometric trajectories for several example events resulting from the source trajectories marked in Fig. 4.

From the figures, one finds that $\Delta\delta\theta_c$ is also large for the wide binary lens system in a considerably large area around caustics and the resulting astrometric trajectories have distinctive features. Especially large excess centroid shifts occur in the region along the binary axis. One also finds that the general patterns of $\Delta\delta\theta_c$ in the region around each caustic is similar to those in the region around the central caustic of the narrow binary lens case. That is, the excess centroid shifts diverges from the on-binary-axis cusps and converges towards the off-binary-axis cusps. One major difference is that in the region between the right-side on-binary-axis cusp of the left caustic and left-side on-binary-axis cusp of the right caustic, the combination of the two diverging excess centroid shift vectors from the individual cusps makes $\Delta\delta\theta_c$ directed almost vertically from the binary axis. As a result, the centroid shift trajectory of an event passing through this region (e.g. part of the trajectory 3 around the moment of the source star’s closest approach to the center of mass) becomes convex compared to the astrometric trajectory of the combined single lensing events. Another interesting deviations occur when the source passes closely both lenses. For this case, the astrometric trajectory will have double bumps or twisted loops

(e.g. the trajectories 1, 2, and 3), which characterize the event is caused by a wide binary.

3.3. Caustic Crossing Event

When binary separation becomes equivalent to θ_E , the separated caustics merge together and form a single large closed caustic encompassing the center of mass of the binary. The caustic has 6 cusps and two of them are located on the binary axis (see Figure 7). Since the size of the caustic is maximized at around this binary separation, events caused by these binaries have high chance of caustic crossings.

To see the astrometric properties of caustic crossing events, we present in Figure 7 the vector field map of a binary lens system with $\ell = 1.0$ and $q = 0.5$. We also present in Figure 8 two example astrometric trajectories (lower two panels) whose source trajectories are marked in the map. Although this binary lens system cannot be well approximated either by a single lens nor by the superposition of the two independent single lenses, we compute the excess centroid shifts by using equation (5). From the figures, one finds the general pattern of the deviation vector in the region inside of the caustic is that $\Delta\delta\theta_c$ converges towards the on-binary-axis cusps and diverges from the off-binary-axis cusps. Note that this pattern is exactly opposite to that of the excess centroid shifts in the region outside of the caustic. As a result, the two adjacent excess centroid shift vectors just inside and outside of the caustic line have opposite directions. When a source crosses the caustic, then, the deviations in the astrometric trajectory becomes very big not only because the absolute value of the centroid shift is very large near the caustics but also the direction of $\Delta\delta\theta_c$ is reversed during the caustic crossing. We note that these patterns of $\Delta\delta\theta_c$ in the region very close to and inside of caustics apply also to caustic regions of the narrow and wide binary lens systems (see the lower panels of Figure 1 and 3). The only exception is the outer caustic of the narrow binary lens system, in which the direction of $\Delta\delta\theta_c$ is not reversed during caustic crossings (see the lower right panel of Fig. 2).

4. Confusion with Other Types of Deviations

In previous section, we illustrate various forms of deviations in the astrometric trajectories caused by the lens binarity. Besides the lens binarity, however, the trajectory can also be distorted due to various other reasons. First, the astrometric trajectory can be distorted by the change of the observer’s location during the event caused by the orbital motion of the Earth around the Sun: parallax effect (Paczynski 1998; Han 2000). Second, if a star not participating in the lensing process is located too close to the source star (not the lens) to be resolved even with a high resolution interferometer, such as a close companion of the source star, the astrometric trajectory can also be distorted: blending effect (Han & Kim 1999). Third, if the size of the source star is not negligible compared to the Einstein ring radius, the astrometric trajectory is distorted: finite source effect (Mao & Witt 1998).

However, the distortions caused by these effects have different forms from those affected by the lens binarity. The trajectory affected by the blending effect has characteristic linear component caused by the displacement towards the blended star [see the example trajectories in Figure 4 of Han & Kim (1999)], and thus can be distinguished from the trajectories affected by the lens binarity. The deviation caused by the parallax effect is periodic with a known period of a year, allowing one to notice the effect. The deviations caused by the finite source effect is somewhat confusing because it can produce concave and twisting distortions similar to those of binary lensing events. However, the resulting astrometric trajectories of events affected by the finite source effect are exactly symmetric with respect to the semi-minor axis of the unperturbed elliptical trajectory. On the other hand, the astrometric trajectories of binary lensing events are asymmetric in general, and thus one can distinguish the two types of astrometric deviations.

5. Summary

The findings about the astrometric properties of binary lensing events from the analysis of the vector field maps of excess centroid shifts for various types of binary lens systems are summarized as follows.

1. The lens binarity causes large deviations in the astrometric trajectory from the elliptical one of a single lensing event. The excess centroid shifts are substantial even in the regions considerably away from the caustics, implying that the distortions will be significant even for a significant fraction of non-caustic crossing binary lensing events.
2. Depending on the locations with respect to lens caustics, the excess centroid shifts have very characteristic sizes and directions. As a source passes through these regions, the resulting astrometric trajectories have distinctive features, which are categorized by concave, convex, and twisting distortions.
3. The binary-lens induced deviations in the astrometric trajectory can be distinguished from those caused by other effects, such as the parallax, blending, and finite source effects.

Therefore, astrometric microlensing observations will be an efficient method to detect events caused by binary lenses and to constrain their parameters with accuracy.

Acknowledgements: This work was supported by grant KRF-99-041-D00442 of the Korea Research Foundation.

REFERENCES

- Afonso, C. 1999, *A&A*, 344, 63
- Alard, C., Mao, S., & Guibert, J. 1995, *A&A*, 300, L17
- Albrow, M., et al. 1996, in *IAU Symp. 173, Astrophysical Applications of Gravitational Lensing* ed. C. S. Kochanek & J. N. Hewit (Dordrech: Kluwer), 227
- Albrow, M., et al. 1999, *ApJ*, 522, 1022
- Alcock, C., et al. 1999a, *ApJ*, 518, 44
- Alcock, C., et al. 1999b, preprint (astro-ph/9907369)
- Alcock, C., et al. 2000, preprint (astro-ph/0002510)
- An, J., Han, C., & Park, S.-H. 2000, in preparation
- Bennett, D. P., et al. 1995, in *AIP Conf. Proc. 336, Dark matter*, ed. Holt, S. S. and Bennett, C. L. (New York: AIP), 77
- Boden, A. F., Shao, M., & Van Buren, D. 1998, *ApJ*, 502, 538
- Chang, K., & Han, C. 1999, *ApJ*, 525, 434
- Colavita, M. M., et al. 1998, *Proc. SPIE*, 3350-31, 776
- Di Stefano, R., & Mao, S. 1999, *ApJ*, 457, 93
- Di Stefano, R., & Perna, R. 1997, *ApJ*, 488, 55
- Di Stefano, R., & Scalzo, R. J. 1999, *ApJ*, 512, 579
- Dominik, M. 1999, *A&A*, 341, 943
- Dominik, M., & Hirshfeld, A. C. 1996, *A&A*, 313, 841
- Gaudi, B. S., & Gould, A. 1997, *ApJ*, 482, 83
- Han, C. 1999, *MNRAS*, 308, 1077
- Han, C. 2000, *MNRAS*, submitted
- Han, C., & Kim, T.-W. 1999, *MNRAS*, 305, 795
- Høg, E., Novikov, I. D., & Polnarev, A. G. 1995, *A&A*, 294, 287
- Jeong, Y., Han, C., & Park, S.-H. 1999, *ApJ*, 511, 569
- Mao, S., & Di Stefano, R. 1995, *ApJ*, 440, 22
- Mao, S., & Witt, H. J. 1998, *MNRAS*, 300, 1041
- Mariotti, J. M., et al. 1998, *Proc. SPIE*, 3350-33, 880
- Miralda-Escudé, J. 1996, *ApJ*, 470, L113
- Miyamoto, M., & Yoshii, Y. 1995, *AJ*, 110, 1427
- Paczyński, B. 1998, *ApJ*, 404, L23
- Pratt, M., et al. 1996, in *IAU Symp. 173, Astrophysical Applications of Gravitational Lensing* ed. C. S. Kochanek & J. N. Hewit (Dordrech: Kluwer), 221

- Rhie, S. H., & Bennett, D. P. 1996, *Nucl. Phys. Proc. Suppl.*, 51B, 86
- Udalski, A., Kubiak, M., & Szymański, M. 1997, *Acta Astron.*, 47, 319
- Udalski, A., Szymański, M., Mao, S., Di Stefano, R., Kaluzny, J., Kuniak, M., Mateo, M., & Krzemiński, W. 1994, *ApJ*, 436, 103
- Unwin, S., Boden, A., & Shao, M. 1997, in *AIP Proc. 387, Space Technology and Applications International Forum 1997*, ed. M S. El-Genk (New York: AIP), 63
- Walker, M. A. 1995, *ApJ*, 453, 37
- Witt, H. 1990, *A&A*, 263, 311

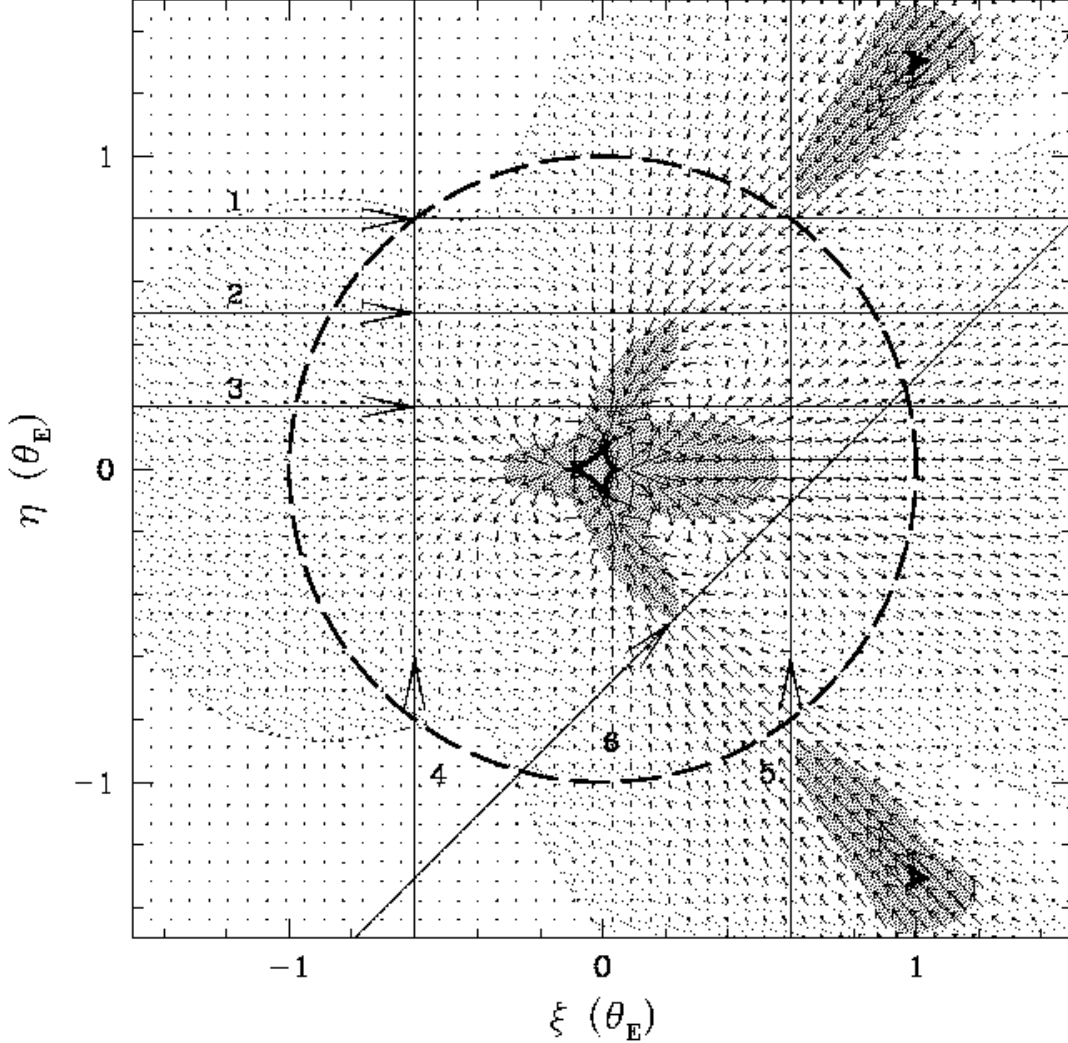


Figure 1: Vector field map of the excess centroid shifts for an example narrow binary lens system with a separation $\ell = 0.5$ and a mass ratio $q = 0.2$. The positions are chosen so that the center of mass is at the origin. Both lenses are located on the ξ axis and the heavier lens is to the right. The circle drawn with a long-dashed line represents the combined Einstein ring. The three closed figures drawn by thick line are caustics. Also drawn are the contours of the absolute values of the excess centroid shift, $\Delta\delta\theta_c$. The contours are drawn at the levels of $\Delta\delta\theta_c = 0.02\theta_E$ (dotted line) and $0.2\theta_E$ (solid line). The straight lines with arrows represent the source trajectories whose resulting light curves and astrometric trajectories are presented in Fig. 3.

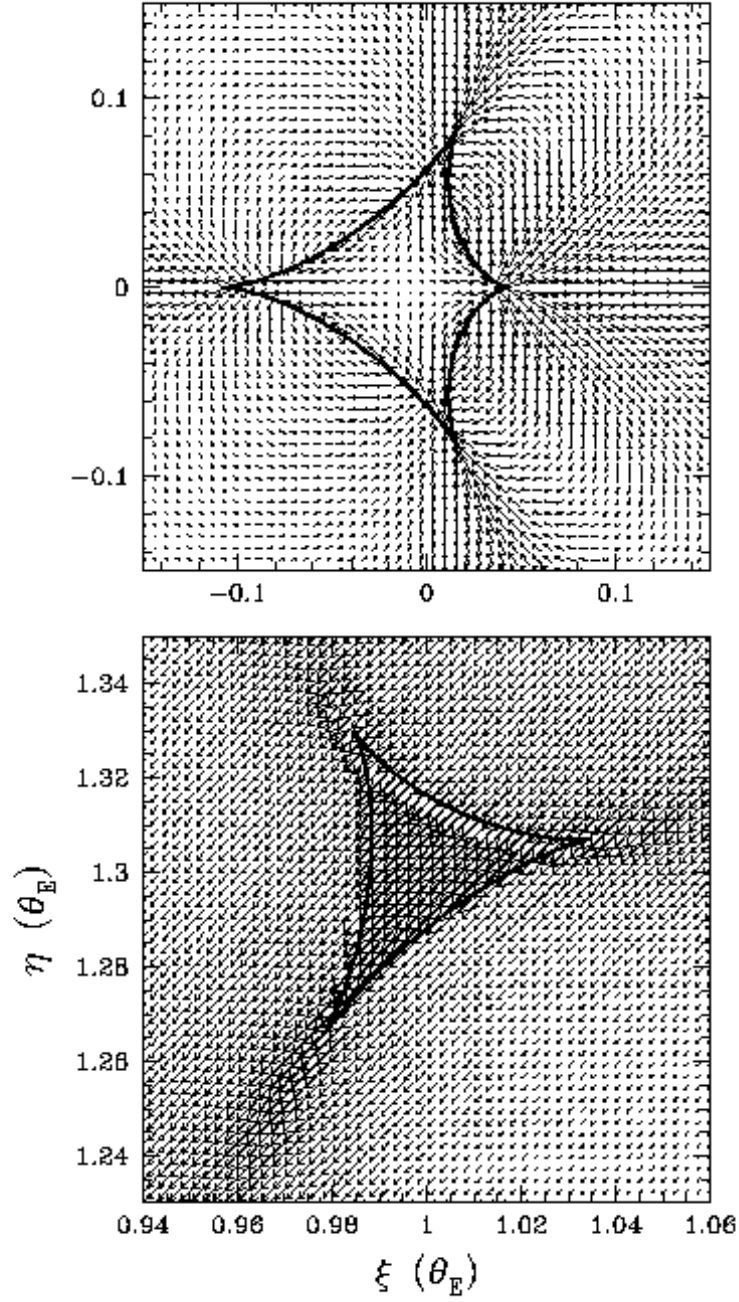


Figure 2: Vector field map of the excess centroid shifts in the region near the caustics of the same lens system as in Fig. 1. The upper and the lower panels are for the central and the outer caustic regions, respectively

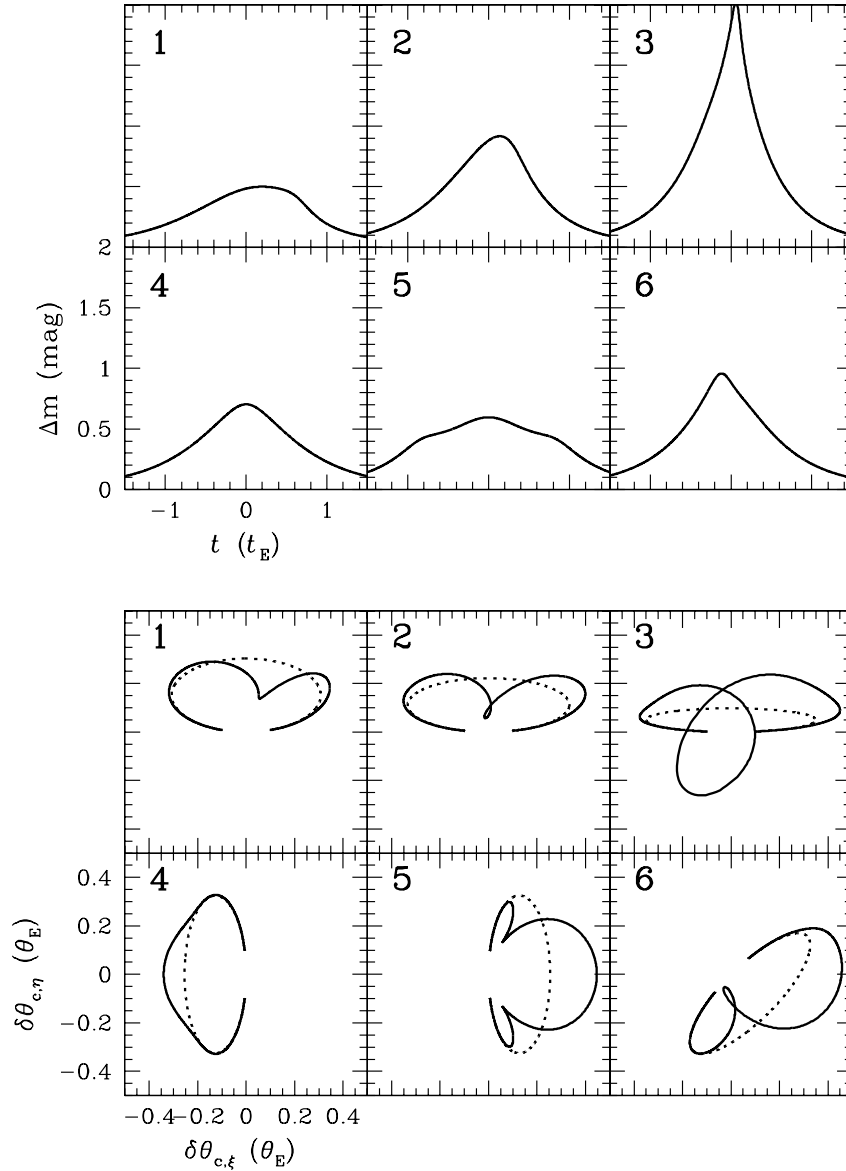


Figure 3: Light curves (upper 6 panels) and astrometric trajectories (lower 6 panels) for several example non-caustic crossing narrow binary lensing events whose source trajectories are marked in Fig 1. The number in each panel matches with the number of the corresponding source trajectory in Fig. 1. The dotted curve in each of the lower set of panels represents the astrometric trajectory of a single lensing event with a mass equal to the total mass of the binary and located at the center of mass of the binary.

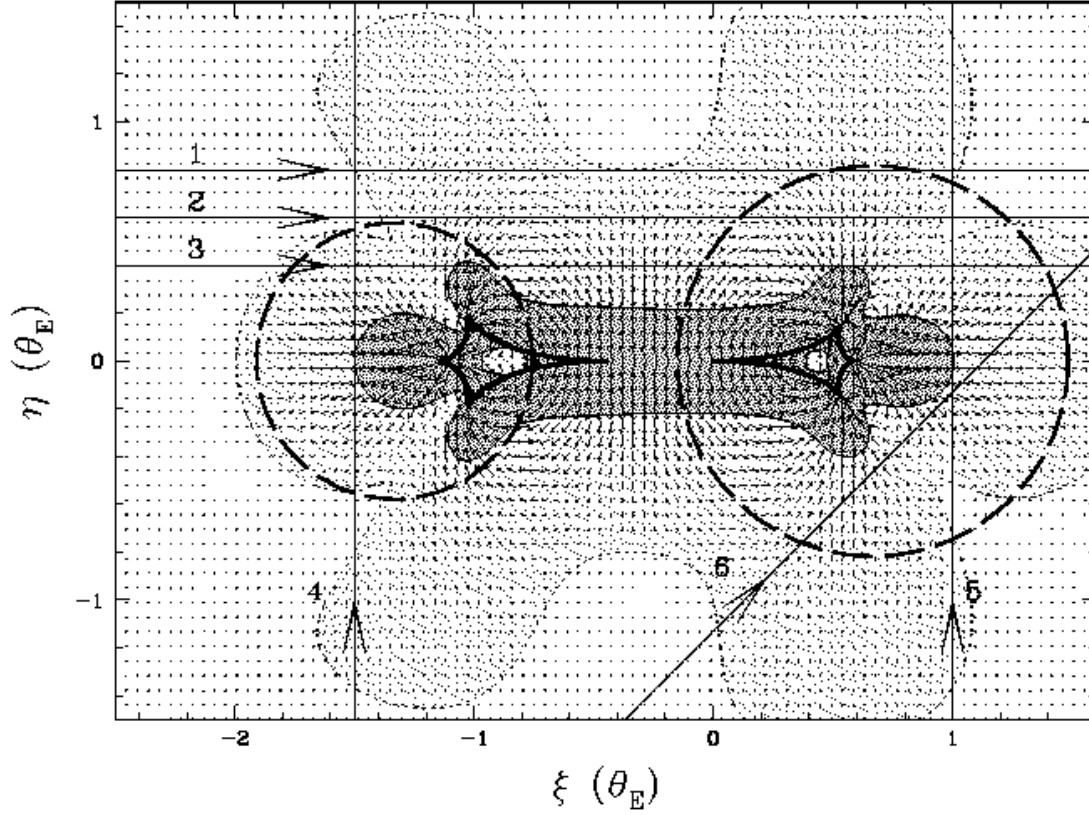


Figure 4: Vector field map of the excess centroid shifts for an example wide binary lens system with a separation $\ell = 2.0$ and a mass ratio $q = 0.5$. The two circles drawn by a long-dashed line represent the Einstein rings of the individual single lenses. The positions and notations are same as those in Fig. 1.

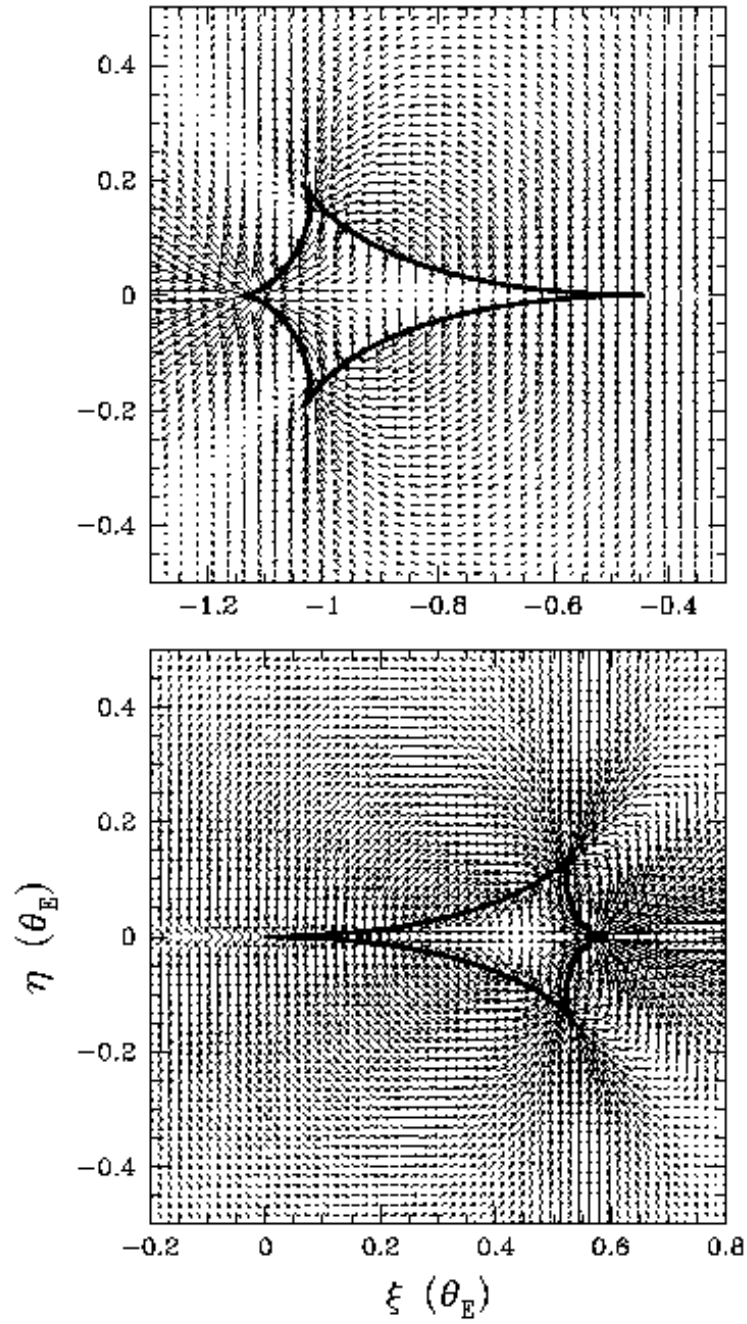


Figure 5: Vector field map of the excess centroid shifts in the region near the caustics of the same lens system as in Fig. 4.

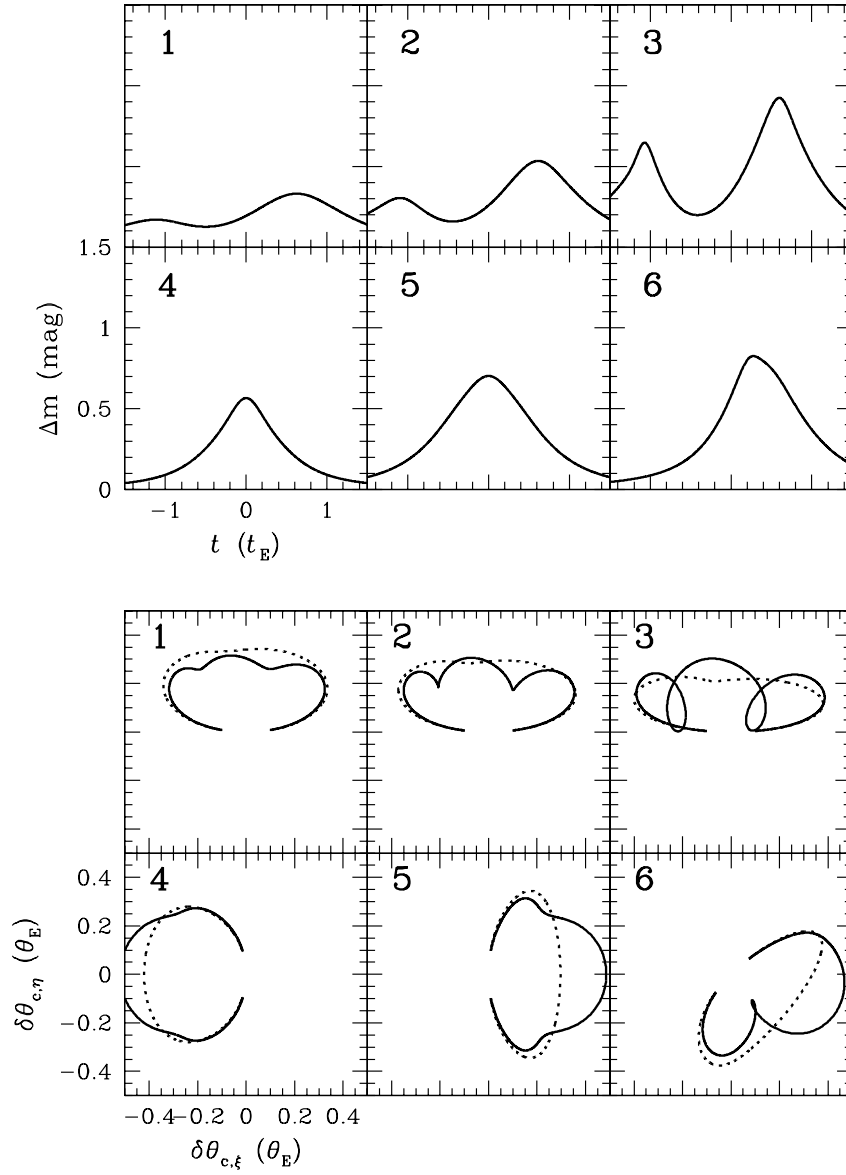


Figure 6: Light curves (upper 6 panels) and astrometric trajectories (lower 6 panels) for several example non-caustic crossing wide binary lensing events whose source trajectories are marked in Fig. 4. The notations are same as those in Fig. 3.

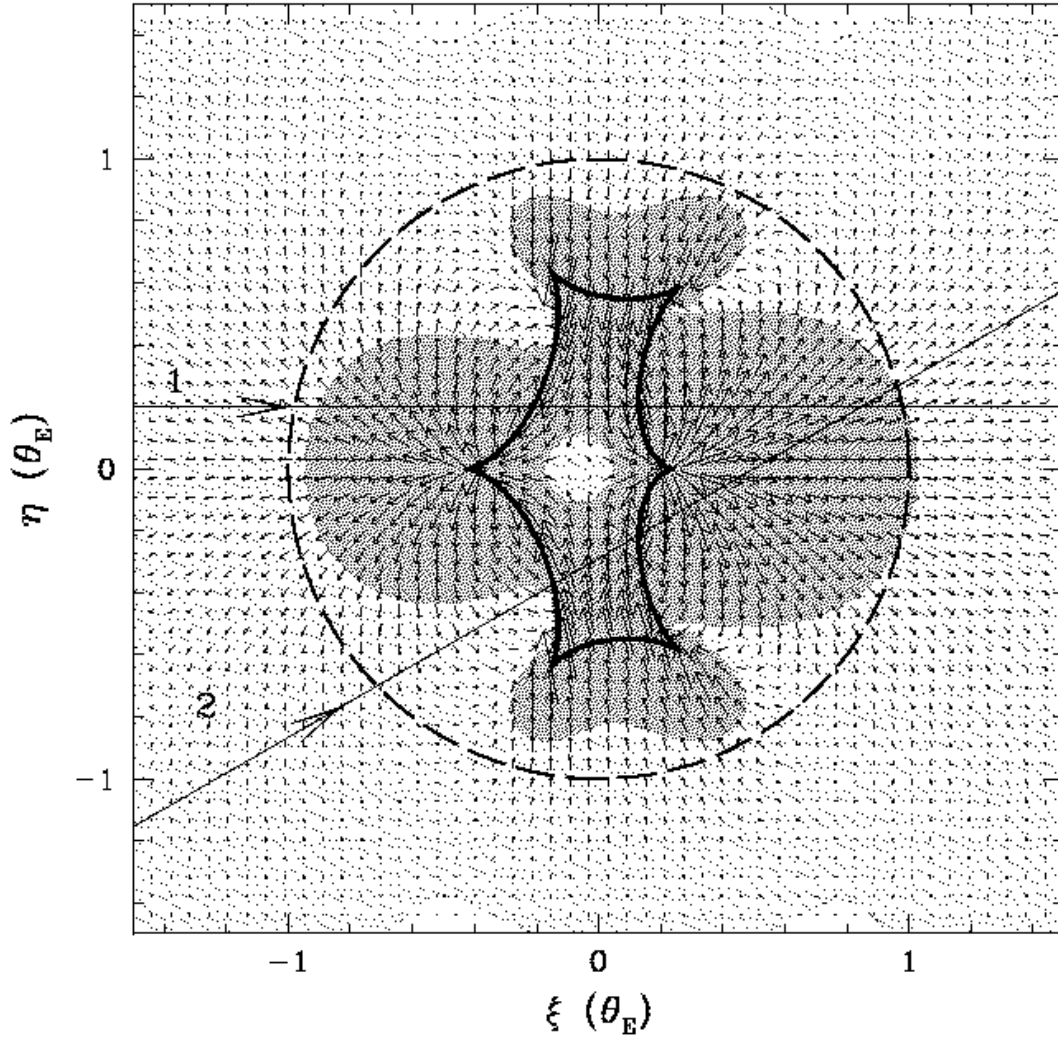


Figure 7: Vector field map of the excess centroid shifts for a binary lens system with $\ell = 1.0$ (upper panel) and $q = 0.5$. The notations are same as those in Fig. 1.

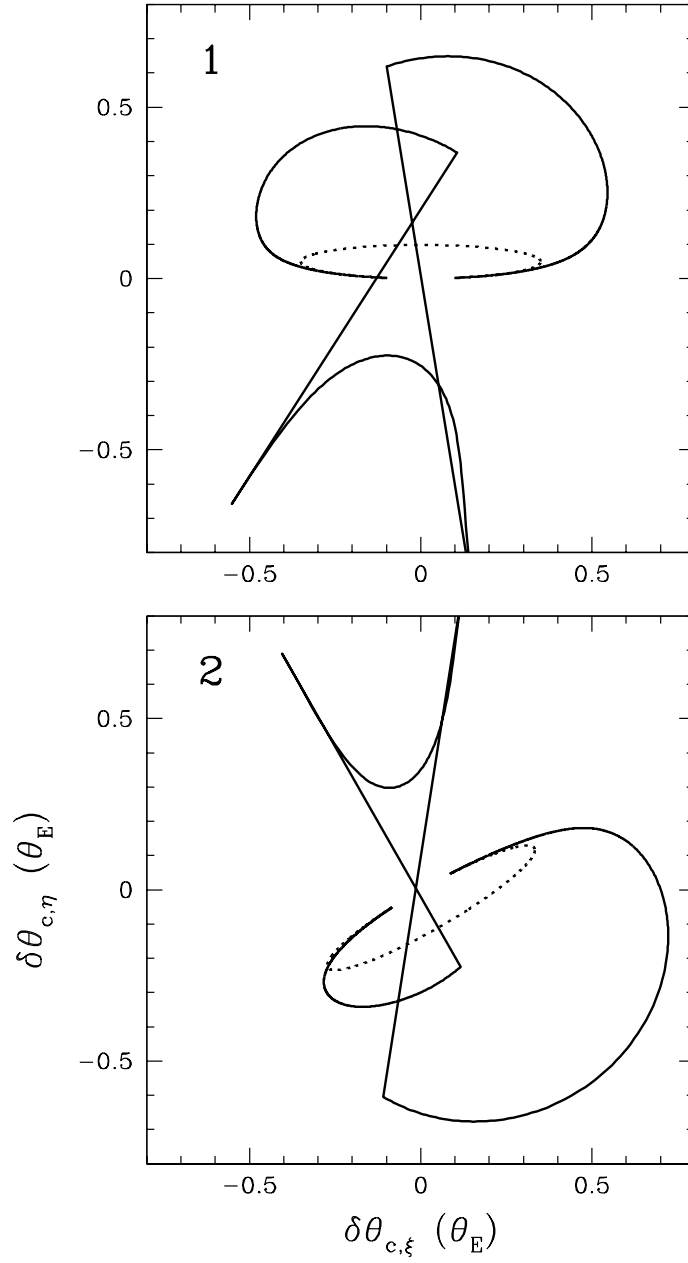


Figure 8: The astrometric trajectories of caustic crossing events whose source trajectories are marked in Fig 7. The dotted curves are the corresponding single lensing events.